



Published in final edited form as:

Dent Mater. 2018 February ; 34(2): 192–200. doi:10.1016/j.dental.2017.10.003.

3D Printed Versus Conventionally Cured Provisional Crown and Bridge Dental Materials

Anthony Tahayeri^{#,1}, MaryCatherine Morgan^{#,1}, Ana P. Fugolin¹, Despoina Bompolaki¹, Avathamsa Athirasala¹, Carmem Pfeifer¹, Jack Ferracane¹, and Luiz E. Bertassoni^{*,1,2,3}

¹Division of Biomaterials and Biomechanics, Department of Restorative Dentistry, School of Dentistry, Oregon Health & Science University, Portland, OR, USA

²Department of Biomedical Engineering, School of Medicine, Oregon Health & Science University, Portland, OR, USA

³Center for Regenerative Medicine, Oregon Health & Science University, Portland, OR, USA

Abstract

Objectives—To optimize the 3D printing of a dental material for provisional crown and bridge restorations using a low-cost stereolithography 3D printer; and compare its mechanical properties against conventionally cured provisional dental materials.

Methods—Samples were 3D printed (25×2×2 mm) using a commercial printable resin (NextDent C&B Vertex Dental) in a FormLabs1+ stereolithography 3D printer. The printing accuracy of printed bars was determined by comparing the width, length and thickness of samples for different printer settings (printing orientation and resin color) versus the set dimensions of CAD designs. The degree of conversion of the resin was measured with FTIR, and both the elastic modulus and peak stress of 3D printed bars was determined using a 3-point bending test for different printing layer thicknesses. The results were compared to those for two conventionally cured provisional materials (Integrity[®], Dentsply; and Jet[®], Lang Dental Inc.).

Results—Samples printed at 90° orientation and in a white resin color setting was chosen as the most optimal combination of printing parameters, due the comparatively higher printing accuracy (up to 22% error), reproducibility and material usage. There was no direct correlation between printing layer thickness and elastic modulus or peak stress. 3D printed samples had comparable modulus to Jet[®], but significantly lower than Integrity[®]. Peak stress for 3D printed samples was comparable to Integrity[®], and significantly higher than Jet[®]. The degree of conversion of Integrity[®] also appeared higher than that of 3D printed samples or Jet[®].

*Corresponding author: bertasso@ohsu.edu, Permanent Address: 2730 SW Moody Ave, Portland, OR 97210, Phone contact information: (503) 494-8763.

[#]These authors contributed equally to this work

Publisher's Disclaimer: This is a PDF file of an unedited manuscript that has been accepted for publication. As a service to our customers we are providing this early version of the manuscript. The manuscript will undergo copyediting, typesetting, and review of the resulting proof before it is published in its final citable form. Please note that during the production process errors may be discovered which could affect the content, and all legal disclaimers that apply to the journal pertain.

Significance—Our results suggest that a 3D printable provisional restorative material allows for sufficient mechanical properties for intraoral use, despite the limited 3D printing accuracy of the printing system of choice.

Keywords

3D printing; Digital Dentistry; Temporary Crown and Bridge; Provisional Restoration; CAD/CAM

1. Introduction

Rapid and automated prototyping of dental materials and restorations in three dimensions (3D) has had a significant impact in the field of restorative dentistry in recent years¹. The enormous progress of digital dentistry in the recent decade is undeniable, especially since the advent of CAD/CAM imaging and milling systems, which have literally created a new modality of clinical dentistry². The most recent wave of technological development in digital dentistry revolves around the field of 3D printing³. This has been especially true after the expiration of key patents that have protected various 3D printing methods and manufacturers for many years⁴, and are now available to a wider audience of manufacturers and end users for a fraction of the original cost. With such fast expansion, new 3D printing methods and commercially available products continue to appear abruptly both in the market and in the scientific literature^{5,6}. This makes the classification of current 3D printing methods especially difficult. A simplistic approach to define more common 3D printing technologies may categorize printing systems according to their fabrication process⁷. Under this classification, one may differentiate 3D printing methods under 4 general categories: (1) extrusion printing, (2) inkjet printing, (3) laser melting/sintering, (4) lithography printing. In brief, in extrusion printing, a material is dispensed from a nozzle with computer controlled movement of a 3-axis stage^{8,9}. In inkjet printing, micrometer sized droplets of an ink (typically a photopolymer) are dispensed also using 3-axis stages¹⁰. Laser melting and sintering¹¹, on the other hand, typically do not dispense a material from a nozzle; rather, the high temperature of the laser light is used to either sinter or weld specific regions in a powder bed while a stage moves up or down and the material is added layer-by-layer, thus generating a 3D structure. Lastly, light or lithography printing (which often also use lasers as the light source) use photopolymers that are kept in a Z-axis controlled vat, and the 3D structure results from direct exposition of the polymer to light as the vat or sample holder moves up or down³. On this latter method, two equally common approaches are utilized. In common stereolithography (SLA) printing, which is the method used in this study, a galvano mirror scanner directs the laser light to raster the surface of a vat of monomers, exposing voxels to create 3D polymer structures¹². In digital projection printing (or DMD-DPP, which stand for digital micromirror device-digital projection printing), on the other hand, a set of micromirrors control the on-off actuation of light to polymerize monomers an entire single layer at a time, and as a build platform raises, a 3D polymer structure is created layer-by-layer¹³.

Dentistry is widely acknowledged as one of the fields that can greatly benefit from these 3D printing technologies. However, despite the relatively large number of recent review papers discussing the use 3D printing in dentistry^{1,3,5,6,14}, examples in the literature actually

addressing questions pertaining to parameters defining the characteristics and properties of 3D printed restorative dental materials is strikingly low^{12,15}. Fabrication of surgical guides^{16–18}, diagnostic models¹⁹, occlusal splints²⁰, and a myriad of other applications that are not targeted at printing of direct or indirect intraoral restorative materials are already a clinical reality. These examples, however, have generally used polymers that have little potential for intraoral clinical application due to lack of regulatory approval, and incompatibility of their properties with medium to long-term dental applications. The overarching objective of this work, therefore, was to determine the printability and *in-vitro* performance of a commercially available 3D printable dental material currently marketed for provisional restorations (Crown & Bridge NextDent®) using a relatively low-cost (i.e. compared to CAD-CAM systems) commercially available stereolithography 3D printer (FormLabs1+). We first optimized a set of parameters required to improve printing of the monomers, and then tested the hypothesis that 3D printing enables the fabrication of provisional restorative materials with comparable properties to that of the conventionally used clinical products. There are many types of materials used for provisional restorations, including filled composites and unfilled resins. We contend, however, that the purpose of this study was not to compare the different materials so much as to determine whether the new 3D printed polymers have properties that are in the same range as commercial products that are currently used successfully.

2. Materials and methods

2.1 3D CAD design and 3D printing

Samples were designed using an open source CAD software (FreeCAD v. 0.15) prior to 3D printing. For all experiments, test bars were designed with set dimensions of 25 mm in length and 2 mm in width and thickness. Samples were then saved as .STL files and exported into the 3D printing software (PreForm Software 2.10.3). For all printed specimens supports were set to a density of 1, and a point size of 600 µm.

We then performed a two-step optimization experiment, where we first compared the printing accuracy of bars fabricated with different printing orientations relative to the build platform (0, 15, 45 and 90°). Secondly, after the most optimal printing orientation was determined, we then compared the pre-defined resin parameters that are available in the PreForm Software. These parameters have been pre-optimized by the 3D printer manufacturer to polymerize the different materials that are commercially available from the manufacturer materials list. Each setting is named according to the resin that they have been originally optimized for, and include: white, black, grey, clear, tough, flex and castable. For experiments determining the accuracy of printed bars relative to printing orientation, we set the printing layer thickness to 100 µm and used the resin parameter “white”. For experiments testing printing accuracy versus resin parameter, we set the printing layer thickness to 100 µm and used a printing orientation of 90°. 3D printed samples had residual surface monomer cleaned using a laboratory wipe and support structures were clipped flush with the printed structure prior to measurement with calipers. Measurements were made remote from the support structures.

A commercially available unfilled provisional crown and bridge material (NextDent C&B, Vertex Dental, Netherlands) was used for the 3D printing experiments using each of the different printer settings described above. For comparison we utilized two commercial products conventionally used for provisional restorations, namely Integrity[®] (Dentsply, CA) and Jet[®] (Lang Dental Inc., IL)

2.2 3D printing accuracy

3D printing accuracy was determined by comparing the dimension of the printed bars against the dimensions set in the CAD designs. Measurements were performed using a digital caliper (± 0.1 mm) for the length, width and thickness of the 3D printed samples. At least 3 samples were measured per condition tested, and 3 measurements were made within different thirds along the printed bars, except for length, where a single measurement was made per sample. To quantify printing accuracy, we normalized the error of printing by the set value for each dimension and report the average percent error calculated from all samples.

2.3 Laser intensity

To determine the laser light intensity, we utilized a power meter (Moletron Coherent, Santa Clara CA) positioned inside of the printing chamber. The sensor was then exposed to the laser light continuously for 5 seconds, and data points recorded every 0.3 s. We compared the laser intensity for all resin parameters (white, black, grey, clear, tough, flex, and castable) and printing layer thicknesses (25, 50 and 100 μm) available.

2.4 Mechanical properties

After optimizing orientation, resin settings and laser intensity for 3D printing of the printable resins, we compared the mechanical behavior of the 3D printed bars versus that of two conventional materials designed for provisional crown and bridge restorations (Integrity[®] and Jet[®]). Bars having the same dimensions as the 3D printed samples ($25 \times 2 \times 2$ mm) were fabricated by dispensing the materials in a silicon mold covered with a glass slide on top and bottom, and allowing the materials to cure following the manufacturer's recommendations. Samples were then stored at ambient temperature for 24 hours, had their respective length, width and thickness measured, and the mechanical properties were determined using 3-point bending method, as previously described²¹. The elastic modulus was determined from the slope of the initial linear part of the load-deformation curve according to the ISO 4049 standard. Samples were loaded using a universal test machine (MTS Criterion, Eden Prairie, WI) with a cross-head speed of 0.5 mm min^{-1} (N=6).

2.5 Degree of conversion (DC)

Representative measurements of degree of conversion were based on the methacrylate =CH₂ absorption at 6165 cm^{-1} in near-infrared (NIR) transmission spectroscopy²². Prior to IR analyses, samples were cleaned from residual uncured surface monomer using a laboratory wipe, and after 24 hours after fabrication included in epoxy resin. Samples were then cross-sectioned and ground down to 200–300 μm thickness. A 2D map of degree of conversion was then generated based on the sequenced analyses of spectra (Fisher Scientific Nicolet

6700 FT-IR) obtained at every 50 μm , using a square beam with a set special resolution of 50 \times 50 μm , along 3 separate lines (20 measurements) on a cross-sectioned surface of each individual specimen. Data from each line was assembled using SigmaPlot 13 (Systat Software Inc, San Jose, CA, USA), and a color histogram created to reflect the percent degree of conversion.

2.6 Statistical analyses

Data within each measurement parameter was analyzed with one-way ANOVA and a Tukey's multiple comparison post-hoc test ($\alpha = 0.05$) using a statistics software (Prism 7, GraphPad, La Jolla CA). Results are reported as average \pm standard deviation, and p values depicted as * for $p < 0.05$, ** for $p < 0.01$, *** for $p < 0.001$ and **** for $p < 0.0001$.

3. Results

Figure 1a–d show the 3D CAD designs for samples in 0, 15, 45 and 90° orientations, while Figure 1e–h shows representative photographs of the respective 3D printed samples. One aspect that is relevant for clinical fabrication of provisional restorations using 3D printers is that generally the 3D printed parts will require a set of supports, as seen in Figure 1a-h. In practice, this means that after sample fabrication, the supports need to be trimmed and polished.

The 3D accuracy of the printer in fabricating samples of a set dimension (Figure 2) was directly correlated with the printing orientation. The percent error for samples that were designed to be printed 25 mm long was small, and ranged from 0.12 – to 2.4%, with no statistical difference between orientations (Figure 2a). The average percent error measured for sample width, on the other hand, was more apparent (Figure 2b). Samples 3D printed at a 90° orientation had the lowest average percent error, followed by those printed at 0, 15 and 45°, where the 90° orientation was significantly lower than the 45° orientation ($p < 0.05$). The printing accuracy measured for the thickness of the printed samples was highest for the 0° orientation group, and was significantly lower than 15, 45 and 90° orientation groups (Figure 2c).

Given the fact that samples 3D printed with a 90° orientation required less supports and hence less post-processing (such as trimming and polishing, which could affect create surface defects on the samples and lead to a decrease in mechanical properties), the following experiments were run with samples printed with a 90° orientation. We then determined the effect of 3D printing our material using the different printing settings available in the machine. Again, we determined the printing accuracy by measuring length, width and thickness of the 3D printed samples and comparing against the dimensions set in the CAD designs. The average percent error in the length (Figure 3a) of 3D printed samples was lower in the white and flex resin settings, and the white group was significantly lower than the castable resin setting group. Sample width (Figure 3b) also showed a significant difference between resin settings, where the white setting had a significantly lower average error than all other groups, except flex, which was actually lower than white. A similar trend was observed for sample thickness (Figure 3c), where the white and flex resin settings had the lowest percent error. The negative value obtained from the flex resin setting means that

the samples were smaller than the pre-defined dimensions set in the CAD designs. Although the flex resin setting resulted in significantly greater accuracy in width, bars printed using this resin parameter also had the lowest reproducibility of printing; several bars did not adhere to the build tray during the printing process, and many had visible signs of delamination between printed layers (Supplementary Figure S1). Therefore, we chose the white resin setting for subsequent experiments.

To gain further insights into how the resin settings affected the polymerization of our material, we measured the laser intensity at each one of the settings mentioned above (Figure 4). Interestingly, there is almost a two-fold increase in laser light intensity from the grey resin (20 ± 0.7 mW) to the castable resin (42.3 ± 1.2 mW).

After determining the most convenient printing orientation (90°) and resin setting (white) for our prints, we tested the effect of the Z-axis printing resolution on the mechanical properties of 3D printed bars. There was no statistical difference in elastic modulus (Figure 5a) between samples 3D printed with 25, 50 and 100 μm layer thickness. The peak stress (Figure 5b), on the other hand, was significantly higher for samples 3D printed with 25, and 100 μm layer thickness, in comparison to the 50 μm layer thickness group. The laser light intensity measured increased with increasing layer thickness from 25 (13.4 ± 0.3) to 50 (18.0 ± 0.9) to 100 μm (25.0 ± 0.8) layers (Figure 6). Therefore, we selected the 100 μm layer thickness parameter, in addition to the 90° orientation and white resin setting, to compare the mechanical properties of the 3D printed versus two conventional provisional crown bridge materials (Jet[®] and Integrity[®]).

The elastic modulus (Figure 7a) of the 3D printed samples was significantly lower than that of Integrity, but the same as that of Jet. The peak stress (Figure 7b) of the 3D printed and Integrity samples, on the other hand, were similarly high, and significantly greater than that of Jet.

The degree of conversion maps across the thickness of representative samples from the 3 groups showed interesting results (Figure 8). Three observations are clearly noticeable. First, there was no observable difference in DC for individual printed layers (100 μm). Second, the 3D printed bars appeared to be slightly more polymerized at the “top” (near the printing platform) than at the “base”, although a similar pattern is seen in Jet. Third, all groups showed a heterogeneous pattern of conversion throughout the sample, although Integrity appeared to yield a slightly more homogeneous polymerization than both the 3D printed and the Jet samples.

4. Discussion

There is little doubt that 3D printing has great potential in the field of clinical dentistry. Arguably, one of the procedures that can benefit the most from the recent developments in 3D printing technologies is the fabrication of provisional crowns and bridges. Different from 3D printing of complex, large scale, full-arch structures, like orthodontic appliances²⁰, surgical guides^{16–18}, and dentals casts¹⁴, 3D printing of single unit crowns may be done in as little 10–20 min. Therefore, it is not hard to imagine a clinical situation where the

clinician could prepare a tooth, scan it, send it to a chair-side 3D printer, and proceed with other procedures in the same patient while the crown is being printed. The printed part would be easily separated from the supports and immediately cemented. This can potentially increase productivity in the clinic and allow for a more practical way of making provisional restorations. The technology to enable these procedures is already available on the dental market, however, there currently is a lack of information regarding the performance of both 3D printable dental materials and of 3D printers that are compatible with them. In fact, existing 3D printing companies (i.e. EnvisionTEC and DWS) have traditionally marketed printable dental materials that are only compatible with their respective printing systems. These are often expensive and of limited availability. Nevertheless, the widespread use of low-cost (<\$5,000) 3D printers suggest the need for improved characterization of existing 3D printable dental materials with easy access 3D printing systems, such as the one used here.

Although the process of designing and 3D printing dental materials can be very user friendly, there is a myriad of parameters that can vary from printer to printer, and interfere with the quality of the printed parts depending on the material used. Since stereolithography 3D printing functions by rastering a laser light under a vat filled with the photo-polymerizable monomer^{6,14}, and the emission of light on the incrementally added layers of monomer can influence the quality of the printed part^{6,15}, we first characterized the accuracy of the printed samples relative to the dimensions of the 3D designs. We first optimized the best combination of a number of printing parameters (printing orientation, resin color setting, layer thickness), which we show are relevant to achieve consistent and accurate printing.

Interestingly, the accuracy of the 3D printed materials varied considerably depending on the orientation of the printed part and the area of the structure where accuracy was measured. For instance, when taking into account only the length of the 3D printed samples, the percentage error in the printed structures was limited to less than 2% on average, with samples printed in a 90° orientation being the most accurate. However, the percent error in thickness for the same samples was significantly higher (approximately 20% error) when samples were printed at 90°, in comparison to samples printed with a 0° orientation (approximately 10% error). Of note, during printing of samples set to a 0° orientation, samples are formed by exposing the monomer to light as the samples grow in thickness. When samples are printed with 90° orientation, the same process occurs, however, the samples grow in length. Since the length of the samples was not significantly affected by printing orientation, this indicates that the lateral resolution of the laser light is the rate limiting factor preventing more accurate printing of the tested material. Another possibility is that the printing error for this particular material is consistent within a certain range, which we estimate to be approximately 500 μm. If this is the case, then the relative percent error for a dimension originally set to 2 mm will be very high, whereas for a dimension set to 25 mm it will be comparatively low.

Another interesting observation was that a percent error variation greater than 41.5% was observed in sample thickness depending upon which resin color setting was selected for the printing process (Figure 3c). The two resin color settings that yielded the most accurate

prints were white and flex; however, flex was the only resin color setting that resulted in samples that were smaller than the pre-defined CAD designs. Still, even in the best case scenario for white and flex resin color settings, these error values could be considered high for clinical restorations, especially if accurate margins are desired. Another noteworthy aspect is that the printing precision will vary drastically from one material to another. Samples set to the same dimensions of our printable resins but printed using a control clear resin provided by the printer manufacturer showed outstanding precision (data not shown). Similarly, Alharbi et al reported provisional crowns 3D printed using a 3D printer from the same manufacturer as the dental material itself with a printing accuracy down to 30 μm of the CAD designs¹⁵. In summary, it remains to be tested whether the values obtained with our 3D printing system and material are comparable to results obtained using conventional protocols for manual provisional crown and bridge restorations.

It is unclear what exact hardware parameters manufacturers change for each resin color setting. Nevertheless, if one considers that accuracy in stereolithography printing relies on the controlled penetration of light through a monomer blend down to a certain depth^{23,24}, and prevention of lateral refraction of light outside of the region of interest, then it is reasonable to expect that the first parameter to be manipulated is the laser light intensity. It is also well known that a darker material will require higher intensity to cure greater depths than a fully translucent material. Figure 4 shows that the resin settings for grey, clear and white resins are in the lowest range, whereas black, castable and tough, all resins that contain darker/more opaque pigmentation, have considerably higher laser intensity. Therefore, it is reasonable to postulate that the poorer printing accuracy obtained with these three resin settings may be due to the penetration of light to greater depths than the set layer thickness, which would explain the significantly greater sample thickness in these groups (Figure 3c). Moreover, this illustrates the necessity to optimize printing parameters, such as laser intensity and printing orientation, for each individual material being used; an arduous task if one intends to use commercially available low-cost 3D printers with materials that have not been pre-optimized for that particular device.

The mechanism by which individual layers in a 3D printed material interact can determine its final mechanical performance. For instance, it has been shown that the mechanical properties of printed materials that are anisotropic in nature can be influenced by the printing orientation²⁵. Similarly, it has been proposed that the adhesion between successive layers is weaker than the adhesion within the same layer¹², which is partly true and especially dependent upon the conditions at which polymerization occur, as we have also observed (supplementary figure S1). Alharbi et al¹⁵ showed that a 3D printed interim dental material (Temporalis, DWS), similar to the one we tested here, had higher compressive strength when printed in a 90° orientation than when printed in a 0° orientation. The authors observed that uniaxial compression of the sample led to several microcracks, which appeared to propagate from main cracks formed between layers. Preliminary data generated in our lab (data not shown) indicates that elastic modulus begins to be affected as a function of printing orientation only when samples are printed with a Z-resolution of 25 μm . With that in mind, we hypothesized that the layer thickness could be an important contributor to the mechanical properties of our samples, which were 3D printed with a 90° orientation. Accordingly, if that was the case, the lower the layer thickness, the more layer to layer

interfaces available to affect the mechanical performance. Our results do not support this conjecture, since there was no statistical difference in elastic modulus data for samples printed with 25, 50 and 100 μm layer thickness. Moreover, both 25, and 100 μm layer thickness resulted in higher peak stresses than 50 μm layer thickness, which point towards a different mechanism regulating the mechanical properties of these materials other than layer-layer interaction. In addition, our SEM images of the fractured sites in 3D printed samples did not show layer separation or noticeable microcracks (supplementary figure S2). It is important, however, to state that the mechanical performance of 3D printed dental materials should be carefully examined under anisotropic loading, since a crown or related structure will not encounter strictly uniaxial stresses. This represents an important limitation of the current study which should be carefully considered for future work.

When our 3D printed samples were compared to either Jet or Integrity, two commonly used dental materials for provisional restorations, the elastic modulus of the 3D printed samples was statistically equivalent to that of Jet, but significantly lower than that of Integrity. The peak stress, on the other hand, was similar for integrity and the 3D printed samples, and both were significantly higher than that of Jet. This suggests that both the elastic modulus and peak stress of the 3D printed material were in comparable range to those of Integrity and Jet, which indicates that the 3D printed provisional restorations would have sufficient mechanical properties to be used intra-orally. One important factor that needs to be highlighted is that the manufacturer's recommendation for the printable resin is that these materials should be post-cured in a UV light box and/or in higher temperatures, which we chose not to do in this study. We were particularly interested in testing the properties of the material prior to any post-processing, as we envision that a post-polymerization time (1-2 h) would significantly impact the feasibility of this material for chair-side clinical application. Therefore, it is worth noting that the mechanical performance of the printed material is likely to increase substantially after post-polymerization, which forms the basis for other studies in our laboratory.

We have extensively characterized the correlation between degree of conversion and mechanical performance of several photopolymerized dental resins²⁶⁻²⁸, and it is well known that a higher DC typically results in a higher elastic modulus. Representative maps of DC comparing the 3D printed samples versus Integrity and Jet show a similar conversion pattern for the printed samples and Jet, whereas a more homogeneous polymerization is observed for integrity. One explanation for the high variability seen in Jet samples may be due to preparation variability for the samples. Importantly, contrary to previous observations in 3D printed provisional materials¹², no apparent difference is seen between printed layers, which supports our observation that no delamination occurred in our loaded bars. Both integrity and jet are self-curing materials, however, integrity has a combination of up to 60% acrylates and methacrylates, including bis- and multifunctional monomers, and up to 40% bariumboroalumino silicate glass, which increases stiffness²⁹. Jet is primarily composed of methyl methacrylate with no other significant additives, such as fillers or catalysts. Similarly, our 3D printed resins are unfilled, and have at least 90% methacrylic oligomers that are photocrosslinked due to the presence of up to 3% phosphine oxides as photoinitiators in the monomer blend²⁹. Therefore, it appears that the lack of filler particles may explain the significantly lower stiffness for both Jet and the 3D printed samples in

comparison to Integrity. However, it is noteworthy that even in the absence of filler particles and without the recommended post-curing, both the elastic modulus and peak stress of the 3D printed samples were within an acceptable range for intraoral use.

5. Conclusion

In this study we characterized the stereolithography 3D printing parameters that affect 3D printing accuracy of a commercially available crown & bridge provisional restorative material. Both printing orientation and resin color setting had an effect on printing accuracy. Resin color setting and printing layer thickness also influenced the laser light intensity. We also found that the 3D printing layer thickness had no significant effect on the mechanical properties of 3D printed provisional resins. Furthermore, we show that 3D printed specimens had comparable elastic modulus to conventional crown & bridge Jet acrylic, but lower than that of Integrity, and higher peak stress than Jet acrylic. In summary, within the limitations of this study, our results suggest that the commercially available 3D printable restorative dental material and 3D printing system used in this study allow for sufficient mechanical properties for intraoral use of provisional restorations, despite the limited 3D printing accuracy. Future work utilizing 3D printing systems that allow for optimization of printing parameters as a function of resin of choice should be performed to improve the accuracy of 3D printed dental materials.

Supplementary Material

Refer to Web version on PubMed Central for supplementary material.

Acknowledgments

The authors acknowledge funding from the National Institute of Dental and Craniofacial Research (NIDCR) and the National Institutes of Health (NIH) (R01DE026170 to LEB), and the Medical Research Foundation of Oregon (MRF to LEB). MCM acknowledges the Apprenticeships in Science & Engineering program at Saturday Academy.

References

1. Abduo J, Lyons K, Bennamoun M. Trends in computer-aided manufacturing in prosthodontics: a review of the available streams. *Int J Dent.* 2014; 2014:783948.doi: 10.1155/2014/783948 [PubMed: 24817888]
2. Mainjot AK, Dupont NM, Oudkerk JC, Dewael TY, Sadoun MJ. From Artisanal to CAD-CAM Blocks: State of the Art of Indirect Composites. *J Dent Res.* 2016; 95:487–495. DOI: 10.1177/0022034516634286 [PubMed: 26933136]
3. van Noort R. The future of dental devices is digital. *Dent Mater.* 2012; 28:3–12. DOI: 10.1016/j.dental.2011.10.014 [PubMed: 22119539]
4. Hornick, J., Roland, D. Many 3D Printing Patents Are Expiring Soon: Here's A Round Up & Overview of Them. 2013. <<https://3dprintingindustry.com/news/many-3d-printing-patents-expiring-soon-heres-round-overview-21708/>>
5. Dawood A, Marti Marti B, Sauret-Jackson V, Darwood A. 3D printing in dentistry. *Br Dent J.* 2015; 219:521–529. DOI: 10.1038/sj.bdj.2015.914 [PubMed: 26657435]
6. Stansbury JW, Idacavage MJ. 3D printing with polymers: Challenges among expanding options and opportunities. *Dent Mater.* 2016; 32:54–64. DOI: 10.1016/j.dental.2015.09.018 [PubMed: 26494268]

7. Obregon F, Vaquette C, Ivanovski S, Hutmacher DW, Bertassoni LE. Three-Dimensional Bioprinting for Regenerative Dentistry and Craniofacial Tissue Engineering. *J Dent Res*. 2015; 94:143S–152S. DOI: 10.1177/0022034515588885 [PubMed: 26124216]
8. Panwar A, Tan LP. Current Status of Bioinks for Micro-Extrusion-Based 3D Bioprinting. *Molecules*. 2016; 21doi: 10.3390/molecules21060685
9. Chang CC, Boland ED, Williams SK, Hoying JB. Direct-write bioprinting three-dimensional biohybrid systems for future regenerative therapies. *J Biomed Mater Res B Appl Biomater*. 2011; 98:160–170. DOI: 10.1002/jbm.b.31831 [PubMed: 21504055]
10. Napadensky E. RadTech Annual Meeting.
11. Ayyildiz S. The place of direct metal laser sintering (DMLS) in dentistry and the importance of annealing. *Mater Sci Eng C Mater Biol Appl*. 2015; 52:343.doi: 10.1016/j.msec.2015.03.016 [PubMed: 25953576]
12. Alharbi N, Osman R, Wismeijer D. Effects of build direction on the mechanical properties of 3D-printed complete coverage interim dental restorations. *J Prosthet Dent*. 2016; 115:760–767. DOI: 10.1016/j.prosdent.2015.12.002 [PubMed: 26803175]
13. Zhang AP, et al. Rapid fabrication of complex 3D extracellular microenvironments by dynamic optical projection stereolithography. *Adv Mater*. 2012; 24:4266–4270. DOI: 10.1002/adma.201202024 [PubMed: 22786787]
14. Nayar S, Bhuminathan S, Bhat WM. Rapid prototyping and stereolithography in dentistry. *J Pharm Bioallied Sci*. 2015; 7:S216–219. DOI: 10.4103/0975-7406.155913 [PubMed: 26015715]
15. Alharbi N, Osman RB, Wismeijer D. Factors Influencing the Dimensional Accuracy of 3D-Printed Full-Coverage Dental Restorations Using Stereolithography Technology. *Int J Prosthodont*. 2016; 29:503–510. DOI: 10.11607/ijp.4835 [PubMed: 27611757]
16. Di Giacomo GA, Cury PR, da Silva AM, da Silva JV, Ajzen SA. A selective laser sintering prototype guide used to fabricate immediate interim fixed complete arch prostheses in flapless dental implant surgery: Technique description and clinical results. *J Prosthet Dent*. 2016; 116:874–879. DOI: 10.1016/j.prosdent.2016.04.018 [PubMed: 27460326]
17. Di Giacomo GA, et al. Accuracy and complications of computer-designed selective laser sintering surgical guides for flapless dental implant placement and immediate definitive prosthesis installation. *J Periodontol*. 2012; 83:410–419. DOI: 10.1902/jop.2011.110115 [PubMed: 21819249]
18. Giacomo GD, Silva J, Martines R, Ajzen S. Computer-designed selective laser sintering surgical guide and immediate loading dental implants with definitive prosthesis in edentulous patient: A preliminary method. *Eur J Dent*. 2014; 8:100–106. DOI: 10.4103/1305-7456.126257 [PubMed: 24966755]
19. Salmi M. Possibilities of Preoperative Medical Models Made by 3D Printing or Additive Manufacturing. *J Med Eng*. 2016; 2016:6191526.doi: 10.1155/2016/6191526 [PubMed: 27433470]
20. Salmi M, Paloheimo KS, Tuomi J, Ingman T, Makitie A. A digital process for additive manufacturing of occlusal splints: a clinical pilot study. *J R Soc Interface*. 2013; 10:20130203.doi: 10.1098/rsif.2013.0203 [PubMed: 23614943]
21. Bacchi A, Nelson M, Pfeifer CS. Characterization of methacrylate-based composites containing thio-urethane oligomers. *Dent Mater*. 2016; 32:233–239. DOI: 10.1016/j.dental.2015.11.022 [PubMed: 26764173]
22. Stansbury JW, Dickens SH. Determination of double bond conversion in dental resins by near infrared spectroscopy. *Dent Mater*. 2001; 17:71–79. [PubMed: 11124416]
23. Urrios A, et al. 3D-printing of transparent bio-microfluidic devices in PEG-DA. *Lab Chip*. 2016; 16:2287–2294. DOI: 10.1039/c6lc00153j [PubMed: 27217203]
24. Bhattacharjee N, Urrios A, Kang S, Folch A. The upcoming 3D-printing revolution in microfluidics. *Lab Chip*. 2016; 16:1720–1742. DOI: 10.1039/c6lc00163g [PubMed: 27101171]
25. Kulkarni P, Marsna A, Dutta D. A review of process planning techniques in layered manufacturing. *Rapid Prototype Journal*. 2000; 6:18–35.
26. Albuquerque PP, Bertolo ML, Cavalcante LM, Pfeifer C, Schneider LF. Degree of conversion, depth of cure, and color stability of experimental dental composite formulated with

- camphorquinone and phenanthrenequinone photoinitiators. *J Esthet Restor Dent.* 2015; 27(Suppl 1):S49–57. DOI: 10.1111/jerd.12131 [PubMed: 25886091]
27. Guimaraes T, Schneider LF, Braga RR, Pfeifer CS. Mapping camphorquinone consumption, conversion and mechanical properties in methacrylates with systematically varied CQ/amine compositions. *Dent Mater.* 2014; 30:1274–1279. DOI: 10.1016/j.dental.2014.08.379 [PubMed: 25249004]
28. Pfeifer CS, et al. Characterization of dimethacrylate polymeric networks: a study of the crosslinked structure formed by monomers used in dental composites. *Eur Polym J.* 2011; 47:162–170. DOI: 10.1016/j.eurpolymj.2010.11.007 [PubMed: 21499538]
29. Thomé, T., et al. *Advanced Polymers in Medicine.* Puoci, F., editor. Springer; 2015.

Highlights

- Provisional crown and bridge resins were 3D printed using a low-cost stereolithography 3D printer
- The elastic modulus and peak stress of 3D printed samples was comparable or higher than that of Jet[®]
- Temporary crowns can be 3D printed with adequate mechanical properties for intraoral use

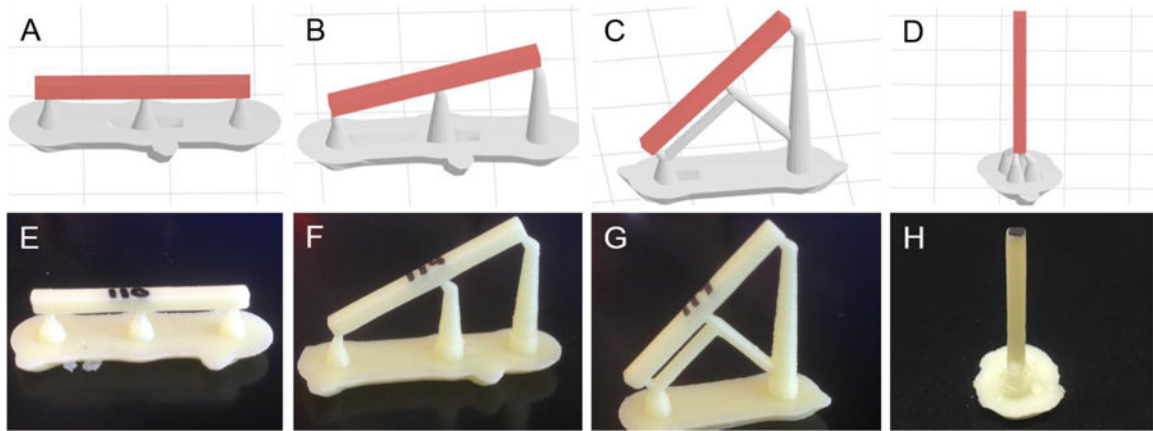


Figure 1. CAD designs for test specimens at (A) 0, (B) 15, (C) 45 and (D) 90° printing orientations. Corresponding polymer structures 3D printed at (E) 0, (F) 15, (G) 45 and (H) 90° printing orientations.

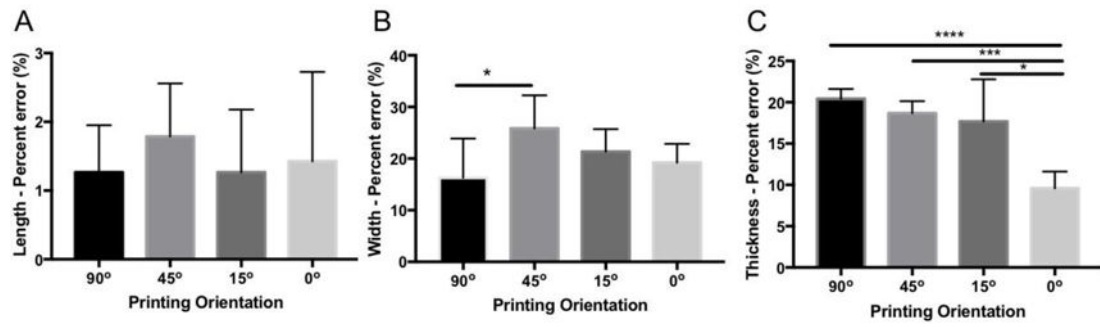


Figure 2. Printing accuracy in (A) length, (B) width and (C) thickness as a function of orientation of the printed bar. Samples were printed using the “white” resin setting and 100 μ m layer thickness. The columns connected by bars were significantly different.

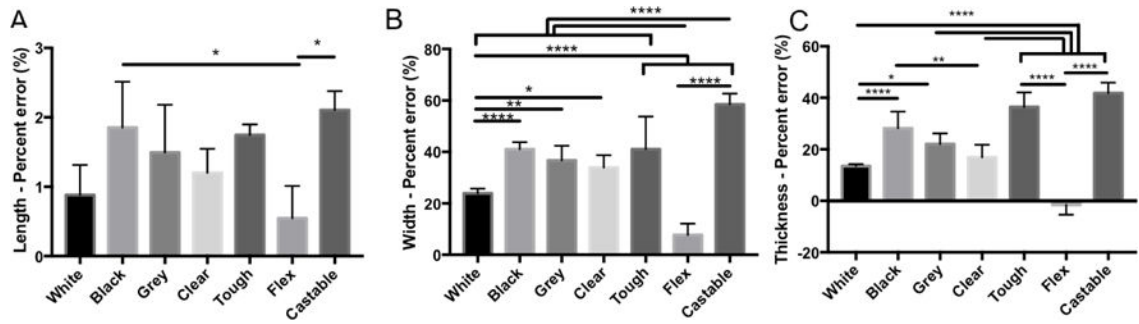


Figure 3. Printing accuracy in (A) length, (B) width and (C) thickness relative to resin color setting. Samples were 3D printed with 100 μm layer thickness and at 90° orientation. The columns connected by bars were significantly different.

Author Manuscript

Author Manuscript

Author Manuscript

Author Manuscript

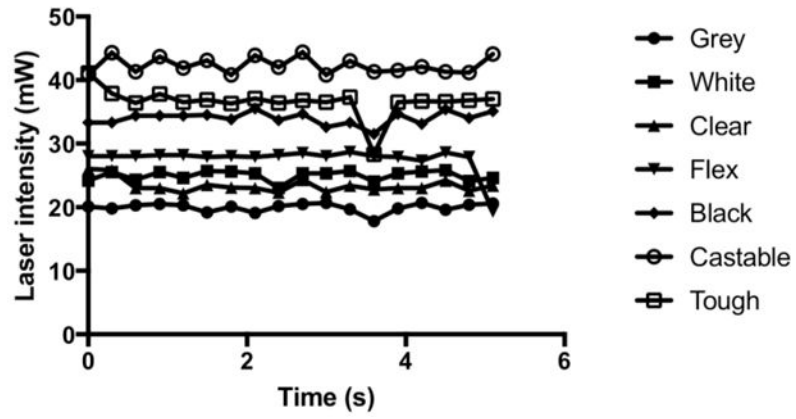


Figure 4.
Laser intensity for different resin color settings.

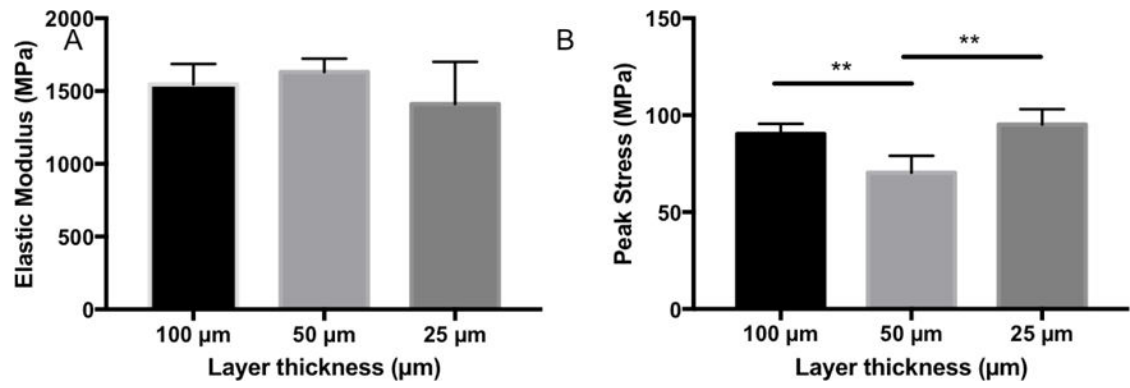


Figure 5.
Mechanical properties for samples 3D printed with 25, 50 and 100 μm layer thickness.

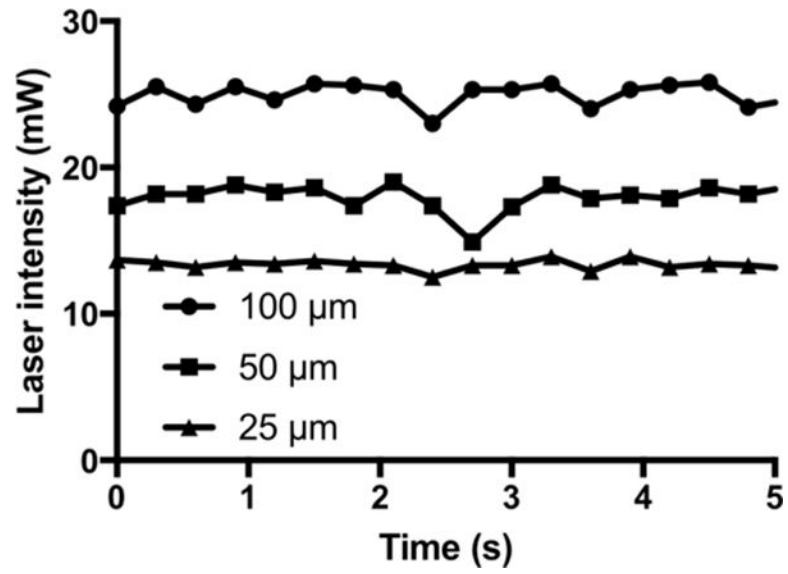


Figure 6. Laser intensity for 25, 50 and 100 μm layer thickness printing parameter.

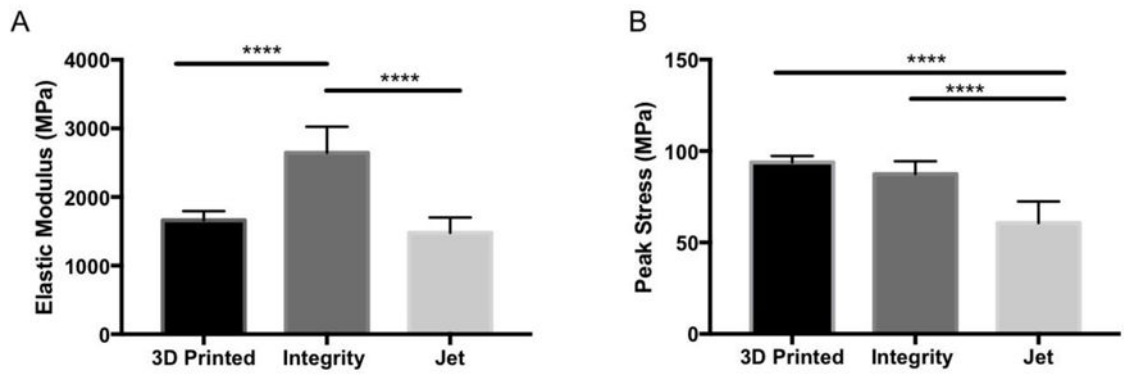


Figure 7.

(A) Elastic modulus and (B) peak stress for 3D printed specimens versus Integrity and Jet specimens.

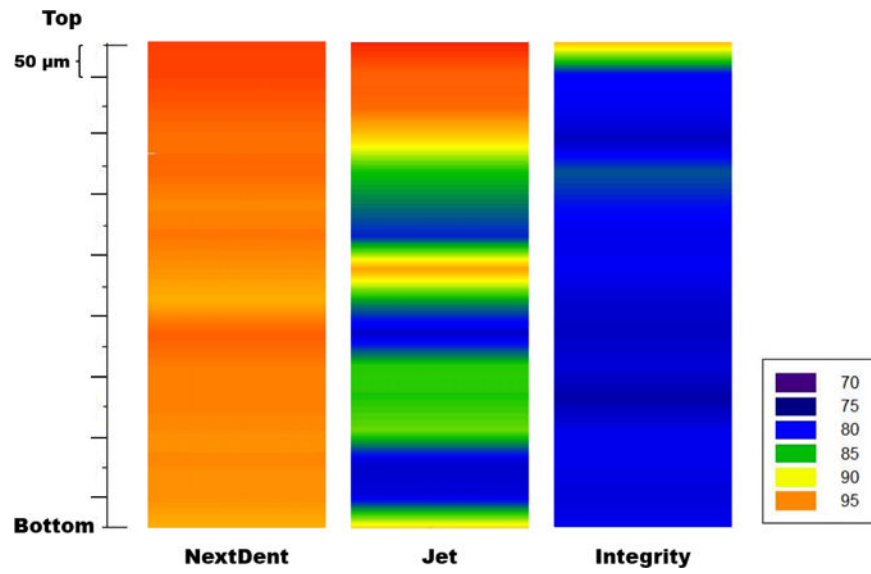


Figure 8. Representative 2D mapping of degree of conversion generated based on spectra obtained at every 50 μm along 3 separate lines (20 measurements in y) on a cross-sectioned surface of each individual specimens.